FUNDAMENTAL TESTS ON STRUCTURAL HEALTH MONITORING SYSTEMS BY USING RFID TAG WITH SENSORS

Akinori Tani[1], Yuichiro Yamabe[2], Masashi Murakami[3] and Motoki UGAJI[4]

[1] *Professor, Dept. of Architecture, Graduate School of Eng., Kobe University, Kobe, Japan*
[2] *Research Associate, Dept. of Architecture, Graduate School of Eng., Kobe University, Kobe, Japan*
[3] *Graduate Student, Dept. of Architecture and Civil Eng., Graduate School of Science and Technology, Kobe University, Kobe, Japan*
[4] *Graduate Student, Dept. of Architecture, Graduate School of Eng., Kobe University, Kobe, Japan*
E-mail: tani@arch.kobe-u.ac.jp, yamabe@kobe-u.ac.jp

ABSTRACT:

As described in this paper, to clarify the applicability of RFID tags with sensors to structural health monitoring systems, fundamental tests were carried out using RFID tags with sensors and built-in memory. An alternative system was used because RFID tags with sensors and built-in memory are under development in Japan. This system has almost identical performance to that of RFID tags and data communication is performed by wireless LAN. Sensors such as acceleration sensors and wire strain gages are used for structural health monitoring systems. Fundamental performances of these sensors were clarified through shaking table tests using four-story and two-story specimens. Fundamental characteristics of the proposed system and used sensors, and the applicability of RFID tags with sensors to structural health monitoring systems are discussed and clarified based on results of shaking table tests and Fast Fourier Transform (FFT) analyses.

KEYWORDS: Structural health monitoring, Acceleration sensor, Wire strain gage, Shaking table tests, RFID tag with sensors

1. INTRODUCTION

Recently, global environmental problems are attracting international attention. In building construction fields, changes to circulation-type production systems are strongly demanded. It is necessary to identify structural performance adequately and properly at each stage of a building's life cycle to use structures for a long time. Based on results of analyses, appropriate structural repairs and anti-seismic retrofit methods can be planned. However, structural performance monitoring systems have not been adopted generally in buildings in Japan. Aiming at ubiquitous structural performance monitoring systems, some application systems using wireless sensor networks are applied to monitoring systems of buildings (Center for Embedded Network Sensing (2007), Kurata et al. (2004) and Paek et al. (2005)).

Regarding other ubiquitous information systems, RFID tags are used widely in various fields. In fact, RFID tags have a characteristic that information is moved simultaneously with devices' attached RFID tags. Data stored in built-in memory mounted on RFID tags can be read, written, and updated. Research related to RFID tag applications in building construction and management fields has been proposed using passive-type RFID tags (Takeda et al. (2004) and Kawamura et al. (2005)). Furthermore, active-type RFID tags are used in many fields. Recently, active-type RFID tags with sensors have come onto the market in Japan. However, these tags have no memory and the data collected by sensors are immediately transmitted to a controller. Built-in memory is considered indispensable because high-speed sampling is necessary to perform structural performance monitoring against earthquake and wind loading. When RFID tags with sensors have built-in memories and have internal batteries, data collected by sensors can be stored in built-in memory; stored data can be transmitted later to controllers accurately after observations. Active-type RFID tags with temperature and moisture sensors and built-in memories are available commercially in Japan. The authors have performed fundamental tests using these active-type RFID tags; their applicability to building monitoring systems has been discussed (Tani et al. (2005)).

To apply active-type RFID tags with sensors to structural health monitoring systems, sensors of acceleration, displacement, strain, pressure, and so on are considered useful. Although active-type RFID tags with these sensors and built-in memory are now under development, it is considered that such tags with sensors and built-in

memory present great possibilities as devices for use in structural health monitoring systems. Regarding fundamental studies of active-type RFID tags with acceleration sensors, the authors performed shaking table tests using two-story and four-story specimens (Tani et al. (2007a and 2007b), and Murakami et al. (2007)). For those studies, an alternative system (Microstrain (2008)) was used because active-type RFID tags with acceleration sensors and built-in memory are under development. This alternative system has almost identical performance to that of RFID tags with sensors and built-in memory; data transfers are performed by wireless LAN.

As described in this paper, fundamental studies of acceleration sensors are performed using a four-story specimen (Tani et al. (2007b), and Murakami et al. (2007)). Furthermore, fundamental studies of wire strain gages are performed using two-story specimen (Ugaji et al. 2008). Based on results of shaking table tests, the applicability of active-type RFID tags with acceleration sensors and wire strain gages, along with accuracy of identification results related to structural characteristics are verified and discussed.

2. OUTLINE OF THE RFID TAG SYSTEM WITH SENSORS

Actually, RFID tags are electronic devices using radio frequency identification technologies. The RFID tags have the following special features: 1) small size, 2) stored data in built-in memory, and 3) non-contact communication. Figure 1 depicts a general configuration of an RFID tag with sensors. Regarding the transition method of stored data, a semi-passive type, one of the data transition methods of active-type RFID tags, is used because the battery is not used in data transmission in the semi-passive type. A battery is built into this system to activate sensors; it is not used for data transmission. Therefore, the battery consumption is considered low.

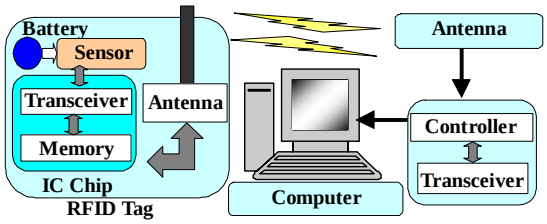

Figure 1 General configuration of RFID tag with sensor and built-in memory

3. OUTLINE OF EXPERIMENTAL SYSTEM

3.1 Experimental System

In Japan, almost all RFID tags with sensors and built-in memory are under development. Therefore, it is difficult to apply those RFID tags to structural health monitoring systems immediately. As described in this paper, an alternative system that offers almost identical performance to that of the RFID tag with sensors and built-in memory is used for this study and data transfers are performed using a wireless LAN. Details of the alternative system used for these tests are shown in Table 1. This alternative system has three analog-digital (AD) converters; moreover, acceleration sensors and wire strain gages can be attached when the sensors have voltage outputs.

Table 1 Details of the alternative system for RFID tags

Communication Frequency	Memory Size	AD Converter	Input and Supply Voltage	Channels of Analog Input
2.4 GHz	2 MByte	12 bit	3 V	3

3.2 Acceleration Sensor and Wire Strain Gage

In earlier papers (Tani et al. (2007a and 2007b)) and in one by Murakami et al. (2007), fundamental shaking table tests using three acceleration sensors were described. As described in this paper, one acceleration sensor, named ‘sensor K’ is used because this sensor is proven to have almost identical performance to that of a servo-type accelerometer. Details of this sensor and the servo-type accelerometer are shown in Table 2.

Table 3 presents specifications of the wire strain gage used here. In this case, output signals are measured as voltages of the Wheatstone bridge produced by the one-gage method. Using measured voltages, strains are

obtained as shown in Eqn. 3.1, in which ε, Δe, E, and Gf respectively denote the strain, output voltage, input voltage, and gage factor. The minimal output voltage becomes about 0.732×10^{-3} V; this output voltage corresponds to about 0.046% strain because the A/D converter of the alternative system is 12 bit.

Table 2 Acceleration sensor sensitivity

Sensor	Rage of Detection (g)	Sensitivity (mV/g)	Error(%)	Supply Voltage (V)
Sensor K	±2	600	±0.1*1	2.7～5.5
Servo-type Accelerometer	±1.7	3000	±0.05*2	～7.0

g: Acceleration of gravity
*1:Non-linearity
*2:Linearity

Table 3 Specification of the wire strain gage used for this study

Gage Length (mm)	Width of Gage (mm)	Gage Factor	Resistance Value	Linear Expansion Coefficeient
5	1.5	2.11±1 %	119.5±0.5 Ω	11×10^{-6} /°C

$$\varepsilon = 4 \cdot \Delta e / (E \cdot Gf) \tag{3.1}$$

3.3 Shaking Table System and Specimens

Photo 1 shows a shaking table system. This system has an 800 × 800 mm shaking table with excitation performance of 1 *g* to 18.6 kgf weight in a single direction. In Photo 1, the alternative system of RFID tags and the servo-type accelerometer are also shown. Figure 2 portrays details of the four-story and two-story specimens. Floors and columns of specimens respectively consist of steel and aluminum plates. For the four-story specimen, response acceleration data are measured on the shaking table and on the fourth floor using sensors and servo-type accelerometers. For the two-story specimen, response acceleration data at the second floor by the sensor and strains of one column at the first floor are measured. Regarding wire strain gages, two gages are attached at both sides of the bottom of the column. Weights and rigidities of each floor are also depicted in Figure 2. The rigidity of each floor are identified using results of shaking table tests and tensile tests on aluminum plates.

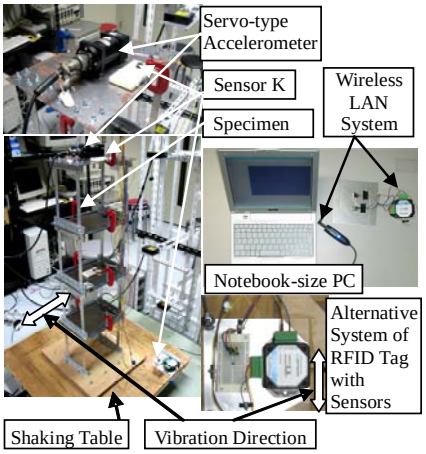

Photo 1 Shaking table test system

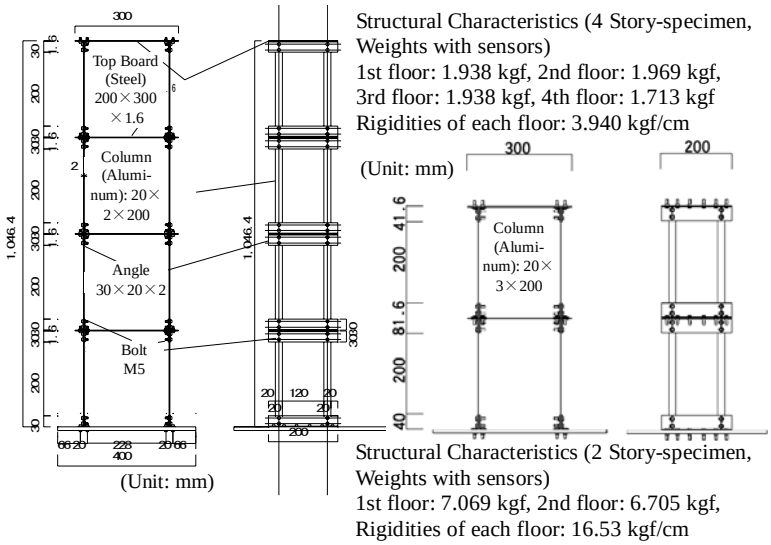

Figure 2 4-story and 2-story specimens

4. MEASUREMENT OF RESPONSE ACCELERATION AND STRAIN

4.1 Accuracy of Employed Sensor

In earlier papers (Tani et al. (2007b), and Murakami et al. (2007)), fundamental shaking table tests were carried out because the sensors were not calibrated. In this section, the accuracy of sensor used for this study is briefly described based on results presented in the earlier papers. Accuracy of detection of amplitudes and phases of observed waves are calibrated with results of sensors and a servo-type accelerometer using sine waves with

frequencies of 2 Hz and 5 Hz. Table 4 shows that four sampling frequencies are used. In these shaking table tests, a sampling interval of activation data to the shaking table and measuring response data was 0.01 s. The duration time was 20 s.

Table 4 Sampling Settings of Sensors

No.	1	2	3	4
Sampling Frequence (Hz)	256	128	64	32
Number of Data	6000	3000	1500	750
Duration Time (s)	23.44			

Table 5 portrays the sensor accuracy in the case of sine wave inputs. In Table 5, the accuracy is calculated using Eqn. 3.2, where A_F, A_{Sensor} and A_{Servo} respectively denote the accuracy of sensors, absolute maximal values of data collected by the sensor, and those collected by the servo-type accelerometer. Superscripts such as 'Max' and 'Min' denote maximal and minimal values of observed data. Scaling factors are also calculated as the mean values of inverse quantities of accuracy of observed results in case of 2 Hz and 5 Hz. Table 6 shows the sensor accuracy for earthquake inputs such as El Centro NS (1940) and JMA Kobe (1995). These results show that the sensor can measure acceleration data on shaking tables accurately in comparison with a servo-type accelerometer when adjustment values on origins and scaling factors are confirmed before measuring accelerations. The effect of phase-lag and sampling frequencies in this sensor is also shown to be small.

$$A\_F = (A_{Sensor}^{Max} / A_{Servo}^{Max} + A_{Sensor}^{Min} / A_{Servo}^{Min}) / 2 \tag{3.2}$$

Table 5 Accuracy of sensor K (Sine wave inputs)

Sensor		Sensor K				Accelerometer
Sampling Frequency		32Hz	64Hz	128Hz	256Hz	
Sin-2Hz	Max(gal)	265	267	277	278	0
	Min(gal)	-269	-275	-272	-277	296
	Accuracy (A_F)	0.93	0.93	0.95	0.96	
Sin-5Hz	Max(gal)	295	322	329	334	0
	Min(gal)	-298	-295	-308	-307	364
	Accuracy (A_F)	0.86	0.90	0.89	0.93	
Scaling Factor		0.86	0.90	0.89	0.93	

$$Scaling\ Factor = \frac{1}{\frac{A\_F_{Sin-2Hz} + A\_F_{Sin-5Hz}}{2}}$$

Table 6 Accuracy of sensor K (Earthquake inputs)

Sensor			Sensor K				Accelerometer
Sampling Frequency			32Hz	64Hz	128Hz	256Hz	
JMA Kobe		Max (gal)	216	213	213	217	216
		Min (gal)	-203	-209	-202	-209	-213
		Accuracy	0.95	1.01	0.99	0.98	
El Centro		Max (gal)	171	170	171	181	220
		Min (gal)	-365	-351	-369	-367	-340
		Accuracy	0.92	0.87	0.96	0.95	
Modified Vale	JMA Kobe	Max (gal)	242	234	233	232	216
		Min (gal)	-228	-230	-222	-223	-213
		Accuracy	1.06	1.11	1.08	1.04	
	El Centro	Max (gal)	192	186	187	193	220
		Min (gal)	-409	-385	-404	-392	-340
		Accuracy	1.03	0.95	1.05	1.01	

4.2 Measurement of Response Accelerations for a 4-Story Specimen

In these shaking table tests, acceleration data of the shaking table and the 4-th floor are collected by sensors and servo-type accelerometers. Displacement data of the shaking table and those of the second and fourth floors of the specimen are collected using laser displacement meters. Regarding earthquake inputs, four earthquake wave models were used: El Centro NS (1940), Taft EW (1952), Hachinohe NS (1968), and JMA Kobe NS (1995). Measurements of sensors were started before the shaking table system was started. They were terminated after the shaking table system was terminated because the system of the shaking table test and the measurement system of sensors could not be synchronized. Regarding the method of superpositioning the observed data, origins of data collected by sensors were shifted horizontally to conform to a clock time of maximal data obtained by servo-type accelerometers and sensors. The sensors' sampling frequency was 128 Hz. The sampling interval on activation data of the shaking table, response data measured by servo-type accelerometers, and laser displacement meters were 0.01 s; the duration time was 20 s. Regarding measurement results, two levels of maximal accelerations of earthquake inputs A_{max} are shown: 1) Case 1, roughly A_{max}=200 gal; 2) Case 2, roughly A_{max}=100 gal as almost half of that of Case 1. Figure 3 portrays comparisons of observed acceleration waves on the shaking table and the 4th floor by the sensor K and the servo-type accelerometer in the case of El Centro and Case 1. Acceleration waves on the 4th floor show relative accelerations from the foundation of the specimen. Fast Fourier Transform (FFT) analyses were performed using relative acceleration waves collected by sensors and servo-type accelerometers. Identified natural periods and average values by FFT analyses are presented in Table 7 with respect to each earthquake input employed for this test. Regarding data collected by servo-type accelerometer, maximal and minimal values on the shaking table and the 4th floor are also presented in Table 7.

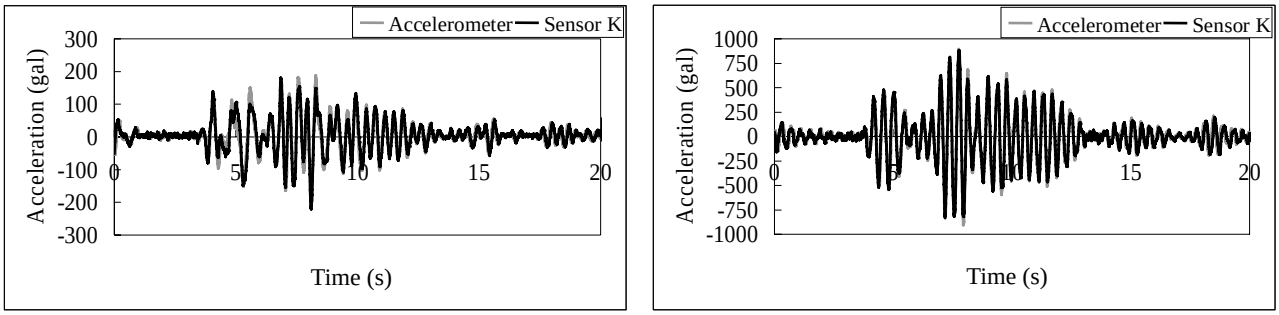

(a) El Centro (on the shaking table) (b) El Centro (on the 4th floor)

Figure 3 Comparisons with data collected by sensor K and servo-type accelerometer in Case 1

Table 7 Identified natural periods of the 4-story specimen

		Servo-type Accelerometer								Senor K			
		Accerelation on the Shaking Table (gal)		Relative Acceleration at the 4th Floor (gal)		Natural Periods(s)				Natural Periods(s)			
		Max	Min	Max	Min	1st	2nd	3rd	4th	1st	2nd	3rd	4th
Case 1	Kobe	188.1	-212.0	894.1	-905.6	0.394	0.146	0.0929	0.0735	0.400	0.147	0.0933	0.0739
	El Centro	148.6	-273.7	622.4	-553.4	0.394	0.147	0.0916	0.0735	0.405	0.147	0.0922	0.0739
	Hachinohe	269.8	-212.5	820.7	-960.8	0.402	0.145	0.0931	0.0737	0.403	0.146	0.0929	0.0752
	Taft	201.6	-169.0	767.7	-794.6	0.394	0.145	0.0929	0.0733	0.395	0.146	0.0930	0.0742
	Average					**0.396**	**0.146**	**0.0926**	**0.0735**	**0.401**	**0.147**	**0.0929**	**0.0743**
Case 2	Kobe	97.3	-102.6	403.3	-433.7	0.398	0.145	0.0927	0.0739	0.400	0.146	0.0933	0.0739
	El Centro	83.7	-131.6	315.1	-259.6	0.394	0.144	0.0916	0.0734	0.395	0.145	0.0920	0.0737
	Hachinohe	134.0	-94.7	423.5	-466.6	0.402	0.145	0.0931	0.0737	0.405	0.145	0.0925	0.0741
	Taft	106.3	-75.7	372.0	-398.8	0.394	0.145	0.0925	0.0737	0.395	0.146	0.0930	0.0741
	Average					**0.397**	**0.145**	**0.0925**	**0.0737**	**0.399**	**0.146**	**0.0927**	**0.0739**

4.3 Sensitivity of Identification of Structural Characteristics based on Data Obtained using a Sensor

Based on results of measurements of acceleration data on the top of the 4-story specimen, the following shaking table tests were performed to clarify the possibility of applying damage detection of buildings after earthquake loading using the sensor employed for this study. Generally, natural periods of damaged buildings are considered to lengthen. Therefore, for these shaking table tests, some weights were added to the top of the 4-story specimen to change the natural period of the specimen. For this study, the following weights of 26 kinds were added to the 4th floor: 19, 28, 56, 80, 107, 130, 154, 182, 210, 238, 275, 306, 334, 362, 390, 434, 462, 490, 518, 546, 584, 606, 634, 662, 690, and 718 gf. In these shaking table tests, the sampling frequency was 128 Hz, and the El Centro NS (1940) model was used. The FFT analyses were performed using relative response accelerations on the 4th floor to the foundation by sensors and servo-type accelerometers, and 1st to 3rd natural periods were identified. Regarding data used for FFT analyses, about 20-s records from modified origins by sensors and all data collected by accelerometers were used. Furthermore, eigenvalue analyses were performed using structural characteristics as shown in Figure 2. For eigenvalue analyses, the 'Frame Method' was used. Figure 4 shows comparisons between FFT and eigenvalue analyses on changes of the 1st to 3rd natural periods related to added weights. In Figures 4(b) and 4(c), modified values obtained by the sensor are shown considering offset values for added weight 0 gf.

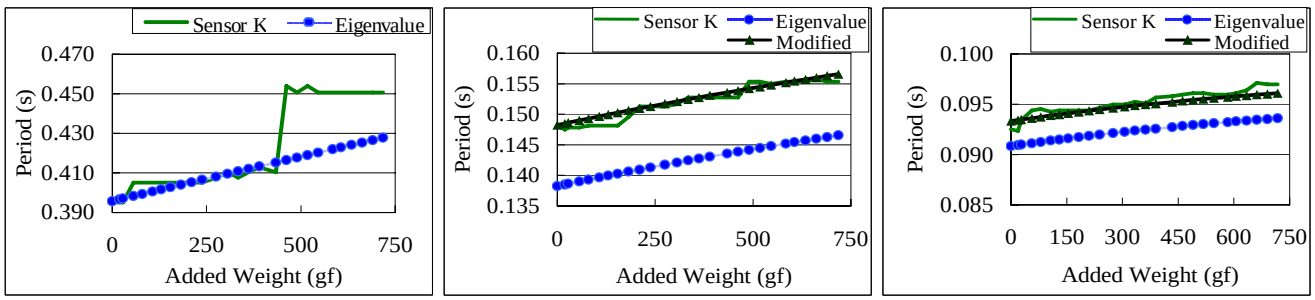

(a) 1st Natural Period (b) 2nd natural period (c) 3rd Natural Period

Figure 4 Changes of natural periods related to added weights in case of FFT and eigenvalue analyses (Case 1)

4.4 Measurement of Strain for the 2-Story Specimen

In shaking table tests, changes of both accelerations at the top of 2-story specimen and strains at the bottom of a column in the 1st floor were measured simultaneously using the alternative system of RFID tag with sensors and built-in memory. Figure 5(a) shows locations of the sensor K and wire strain gages. Regarding wire strain gages, two gages—Gage-1 and Gage-2—were attached at both sides of the bottom of the column in the 1st floor. Each wire strain gage is connected to each Wheatstone bridge circuit, and output voltages are connected to the AD-Input of the alternative system. Figure 5(a) shows that input voltages (3 V) to the Wheatstone bridge circuits are supplied from the alternative system.

Figure 5(b) portrays a result of the static tensile test and assumed bi-linear stress (σ) - strain (ε) relation. Yield strain and stress in assumed bi-linear σ-ε relation are, respectively, about 0.276% and 165 N/mm^2. The sampling frequency of the alternative system is 32 Hz. The Taft EW (1954) model was used as the earthquake input. Regarding maximal accelerations A_{max} on the shaking table, the following two cases were used: Case 3, response displacements are within the elastic range, and A_{max} are about 350 gal; Case 4, response displacements are in the elasto-plastic range and A_{max} are about 750 gal. The duration of earthquake inputs was 20 s. Figure 6(a) shows time historical changes of strain measured using Gage-1 and Gage-2. Figure 6(b) shows an elasto-plastic hysteresis loop calculated using assumed bi-linear σ-ε relationship, as shown in Figure 5(b). Minimal strain by Gage-1 and maximal strain by Gage-2 are, respectively, about -0.355% and 0.318%.

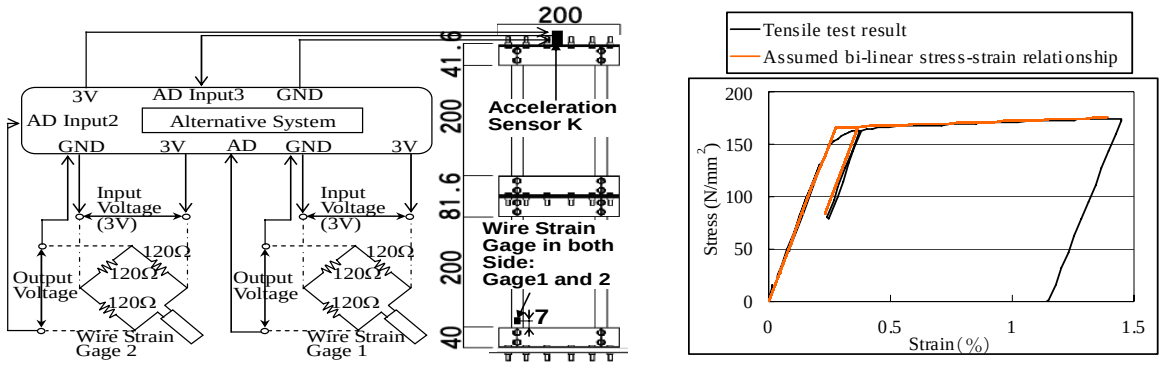

(a) Sensor configuration for the 2-story specimen (b) Tensile test result of aluminum plate

Figure 5 Measurement systems for a 2-story specimen and results of tensile tests

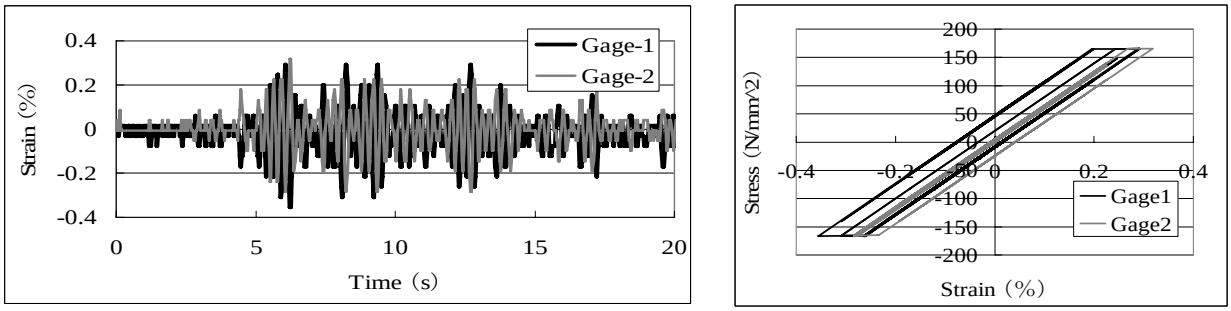

(a) Historical changes of strains (b) Bi-linear hysteresis loops

Figure 6 Time historical changes of strains and bi-linear hysteresis loops (Case 4)

The FFT analyses were performed using time historical data for acceleration and strains; those results are shown in Figures 7(a) and 7(b). Table 8 shows 1st and 2nd natural periods identified by FFT analyses. In Figures 7(a) and 7(b), the 1st and 2nd natural frequencies are identifiable by both the acceleration sensor and the wire strain gage (Gage-2). Table 8 shows that identified values are almost identical. However, the 2nd natural frequency can not be identified in some cases. Figure 7(c) presents the progressive Fourier spectrum using the wire strain gage (Gage-2) for 3.0–4.0 Hz, in which the 1st natural frequency is included. Windows used in progressive FFT analyses were 0–0.5 s, 0–1.0 s,••••,0–29.5 s, and 0–30 s. Figure 7(c) shows that 1st natural frequency becomes small, 5–10 s, and becomes constant for 10–20 s. In this shaking table test, the 1st natural period or frequency is identifiable using FFT analysis, but the 2nd natural period or frequency is unidentifiable.

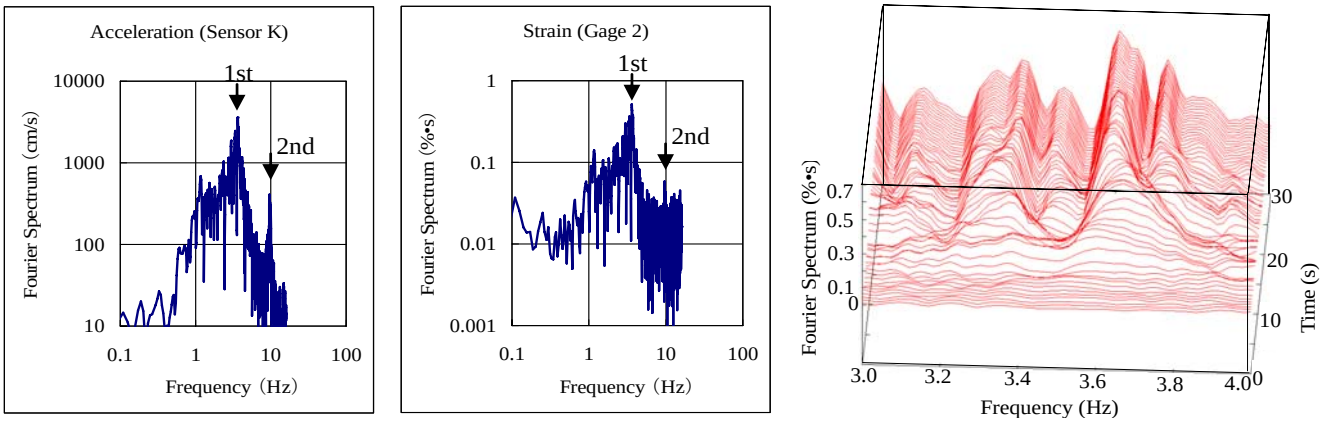

(a) Acceleration (b) Strain by Gage-2 (c) Progressive Fourier spectrum by Gage-2

Figure 7 Results of FFT analyses in case of 2-story specimen (Case 4)

Table 8 Identified natural periods in the case of a 2-story specimen (Unit: s)

	Sensor K		Gage 1		Gage 2	
	Case 3	Case 4	Case 3	Case 4	Case 3	Case 4
1st	0.274	0.277	0.274	0.277	0.275	0.277
2nd	0.102	0.104	Unidentifiable			0.105

Acceleration on Shaking Table		
	Case 3	Case 4
Max	379.7	748.9
Min	-386.0	-678.9

Therefore, it is necessary to improve the proposed system because these phenomena are considered to depend on the measurement accuracy of the proposed system. These results demonstrate that changes of structural characteristics are identifiable using the proposed system and wire strain gages. Furthermore, performance of the proposed system and wire strain gages was verified and clarified.

5. DISCUSSION AND CONCLUSIONS

As described in this paper, aiming at the realization of the ubiquitous health monitoring system on buildings, fundamental tests of performance of acceleration sensors and wire strain gages were performed with shaking table tests. Regarding the ubiquitous sensor system, the alternative system is used because those systems are under development. This system has almost identical performance to that of semi-active type RFID systems with sensors and built-in memory. 4-story and 2-story specimens are used with sensor sampling frequencies of 128 and 32 Hz. Furthermore, FFT analyses were performed to identify natural periods of specimens using data observed with accelerometers and sensors such as acceleration sensors and wire strain gages. Results of shaking table tests and FFT analyses suggest the following conclusions.

1) The acceleration sensor K used in this study can measure acceleration data at the top of specimens and on the shaking table accurately in comparison with servo-type accelerometers when adjustment values of origins and scaling factors are confirmed before measuring acceleration. The effects of phase-lag and sampling frequencies related to data collected by sensor K are considered small.
2) For the 4-story specimen, identification of 1st to 3rd natural periods using FFT analyses can be performed using observed acceleration data accurately. Differences of the identified natural period between the accelerometer and sensor K are small for maximal earthquake inputs to the shaking table of about 200 and 100 gal. Therefore, sensor K is considered applicable as a health monitoring system of buildings when maximal absolute values of earthquake inputs on the ground are greater than 100 gal.
3) Identified 1st to 3rd natural periods by FFT analyses of observed data of sensor K agree with those obtained by eigenvalue analyses. The proposed system is considered applicable to a ubiquitous structural health monitoring system, such as a damage detection system, using observed acceleration data and FFT analyses.
4) Changes of structural characteristics caused by strains of structural members in the plastic range can also be identified using the proposed system and wire strain gages. For the 2-story specimen, the 1st natural period is identifiable by FFT analyses, but the 2nd natural period can not be identified clearly. Regarding the 1st natural period, results identified using wire strain gages agree with those by the acceleration sensor. Further study is necessary to clarify the applicability and accuracy of the proposed system.

5) Based on results obtained through this study, the accuracy of the proposed system, the acceleration sensor used for this study, and the wire strain gage used were verified and clarified. Semi-active type RFID systems with sensors and built-in memory are considered applicable to structural health monitoring systems of buildings. Furthermore, to perform more effective structural health monitoring of buildings, it is necessary to develop damage detection methods for buildings using data collected by sensors.

ACKNOWLEDGEMENT

This study was supported in part by the Twenty-First Century Center of Excellence (COE) Program 'Design Strategy Towards Safety and Symbiosis of Urban Space' awarded to Graduate School of Science and Technology, Kobe University. The Ministry of Education, Culture, Sports, Science and Technology of Japan sponsors the Program.

REFERENCES

Center for Embedded Network Sensing HP. (2007). http://research.cens.ucla.edu/areas/2007/Seismic/projects.htm.

Kawamura, H., Tani, A., Yamabe, Y., Maeno, K., Oku, N., Morimoto, K. and Kyo, D. (2005). Pseudo-Living Recurrent Buildings Composed of Cell Elements With RFID Tags – With Tests on RFID Tag Information System Regarding Timber Monocoque Building: J.Pod System –, Proc. of the 2005 World Sustainable Building Conference in Tokyo, Paper No. 07-005, 2357-2364.

Kurata, N., Spencer, B. F. and Ruiz-Sandoval, M. (2004), Building Risk Monitoring Using Wireless Sensors, Proc. of the 13th World Conference on Earthquake Engineering, CD & DVD-ROM, Paper No. 1406, 1-11.

Microstrain Inc. HP (2008). http://www.microstrain.com/v-link.aspx.

Murakami, M, Tani, A, Yamabe, Y. (2007). Research on Monitoring System for Structure Perform of Building Structures by RFID Tag with Sensors – Applicability of Acceleration Sensor for Identification of Structural Characteristics in Case of Four-Story Specimen –, Proc. of the 30th Symposium on Computer Technology on Information, Systems and Applications, Architectural Institute of Japan, Peer Reviewed Paper, 19-24. (in Japanese)

Paek, J., Chintaiapuid, K., Cafferey, J., Govindan, R. and Masri, S. (2005). A Wireless Sensor Network for Structural Health Monitoring: Performance and Experience, In Proc. of the Second IEEE Workshop on Embedded Networked Sensors (EmNetS-II), 1-10.

Takeda, Y., Munemoto, J., Yoshida, T. and Matsushita, D. (2004). A Study on Goods-Management in Laboratories of University by Using RFID and Data Reference System, Proc. of the 27th Symposium on Computer Technology on Information, Systems and Applications, Architectural Institute of Japan, 43-48. (in Japanese)

Tani, A., Yamabe, Y., Sasaki, Y., Maezono, T., Maeno, K., Oku, N., Tsuji, K., Sugimoto, T. and Kawamura, H. (2005). Experimental Research on Performance-Monitoring of Building Structures by RFID Tags with Sensors - Application to Monitoring of Temperature and Humidity -, Proc. of the 28th Symposium on Computer Technology on Information, Systems and Applications, Architectural Institute of Japan, 127-132. (in Japanese)

Tani, A, Murakami, M, Yamabe, Y. (2007a). Fundamental tests on structural health monitoring systems by RFID tag with acceleration sensors, Proc. of the 2nd International Symposium on Improvement of Structural Safety for Building Structures (ISSBS'06), 28-39.

Tani, A., Murakami, M., Yamabe, Y. (2007b). Fundamental tests on structural health monitoring systems by RFID tag with acceleration sensors – Verification on applicability to structural health monitoring system by 4-story specimen –, Proc. of the 3rd International Symposium on Improvement of Structural Safety for Building Structures (ISSBS'07), 85-94.

Ugaji, M., Tani, A. and Yamabe, Y. (2008). A Health Monitoring System of Building Structures by RFID Tag with Wire Strain Gage – Part 1 Verification on Accuracy of Proposed System -, Annual Meeting of Architectural Institute of Japan, Kinki Branch, Structural Division, Vol. 48, 2008, 41-44. (in Japanese)